ACS APPLIED MATERIALS & INTERFACES

Research Article

www.acsami.org

Stretching and Imaging of Single DNA Chains on a Hydrophobic Polymer Surface Made of Amphiphilic Alternating Comb-Copolymer

Rongrong Liu, Sheau Tyug Wong, Peggy Pei Zhi Lau, and Nikodem Tomczak*

Institute of Materials Research and Engineering, A*STAR (Agency for Science, Technology and Research), 3 Research Link, Singapore 117602

Supporting Information

ABSTRACT: Functionalization of amine derivatized glass slides with a poly(maleic anhydride)-based comb-copolymer to facilitate stretching, aligning, and imaging of individual dsDNA chains is presented. The polymer-coated surface is hydrophobic due to the presence of the long alkyl side chains along the polymer backbone. The surface is also characterized by low roughness and a globular morphology. Stretched and aligned bacteriophage λ-DNA chains were obtained using a robust method based on stretching by a receding water meniscus at pH 7.8 without the need for small droplet volumes or precoating the surface with additional layers of (bio)-molecules. Although the dye to DNA base pairs ratio did not influence substantially the stretching length distributions, a clear peak at stretching lengths close to the contour length of the dsDNA is visible at larger staining ratios.

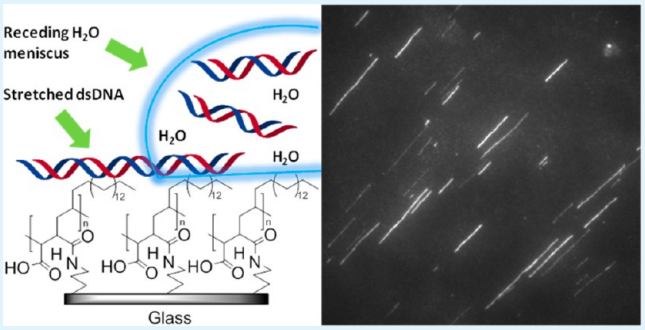

KEYWORDS: *hydrophobic surface, amphiphilic polymer coatings, wide-field microscopy, single DNA imaging, molecular combing, poly(maleic anhydride-alt-1-octadecene)*

1. INTRODUCTION

Visualization and manipulation of single DNA molecules in solution and at interfaces have brought tremendous advances in the understanding of the workings of life's fundamental building block.[1−8] Quantitative high-resolution DNA fiber mapping based on stretching of individual DNA chains[9,10] on surfaces[11] and barcoding the DNA by in situ hybridization[12,13] or by using restriction endonucleases[14−18] allowed evaluating the genetic information on the level of individual DNA chains avoiding the ensemble average information inherent to other techniques e.g. PCR.[19] The chain stretching methods are also suitable for high-throughput analysis of DNA−protein interactions via direct visualization of numerous stretched DNA molecules with bound proteins by fluorescence microscopy.[7]

The methods for DNA stretching include those relying on the hydrodynamic force of a receding droplet meniscus,[20,21] meniscus drying between two surfaces, i.e., molecular combing,[12,22,23] fluid fixation,[17] agarose flow and gel fixation,[24] dynamic molecular combing (based on pulling a slide out from solution),[13] pipet suction,[25] squeezing in nanochannels,[26,27] electric or magnetic fields,[28] or mechanical movement of the meniscus (rather than meniscus motion induced by evaporation).[18] For reliable DNA stretching, for each deposition method, optimization of the solution conditions (pH, presence of salts) and surface chemistry is required. In molecular combing process surface chemistry is most critical to obtain high DNA stretching ratios, and small variation in pH of the DNA solution may affect significantly the length of the stretched DNA.[21,23] When the DNA binds strongly to the substrate via nonspecific interactions the stretching is suppressed and DNA retention, i.e., how many DNA chains attach to the substrate, is high. Decreasing the affinity of DNA to the substrate, on the other hand, may result in high stretching ratios but low retention. Advances in glass surface functionalization methods, such as silanization, allow one to tune the surface properties, e.g., hydrophilicity or charge density. Stretching of DNA have been performed on clean glass,[23] glass coated with vinyl-,[23] and amine-terminated silanes,[12,15,17,18,22,23] polylysine,[16,23] polystyrene,[23] PMMA,[23] polyhistidine,[23] and glass coated with conducting polymers[25] as well as on glass precoated with nontarget single-stranded DNA.[18] For a hydrophobic substrate, it was found that solution pH = 5.5 was optimal, although for some hydrophobic substrates, such as PMMA, PS, or PDMS, the stretching could be also observed for a broad range of pH values.[10] Allemand[23] proposed a model where at pH 5.5 the extremities of the DNA chain are partially melted exposing the hydrophobic core of the helix. This explained also the stronger binding by the chain ends to the surface compared to the midsegment of the DNA. At higher pH values the DNA adsorbed very weakly and was dragged by the receding meniscus resulting in less DNA chains per unit

Received: November 4, 2013
Accepted: January 28, 2014
Published: January 28, 2014

   dx.doi.org/10.1021/am404907c | ACS Appl. Mater. Interfaces 2014, 6, 2479−2485

surface area. On hydrophilic surfaces with ionizable groups the binding and stretching depended on the surface pK_a, and therefore the optimal conditions for which the molecular extension forces would be balanced against electrostatic interactions should have been found for each type of surface separately.

Functionalization of amine derivatized glass slides with reactive poly(maleic anhydride)-based copolymers was shown to be easy and robust.[29−31] In this contribution, we show that a glass slide functionalized with an amphiphilic comb-polymer poly(maleic anhydride-*alt*-1-octadecene) (PMAOD) provides a simple and convenient solution to obtain samples of stretched and aligned bacteriophage λ-DNA. PMAOD coated glass slides have highly hydrophobic character due to the presence of long alkyl side chains, display distinct nanoscale topography and have carboxyl or maleic anhydride groups available for further functionalization. Covalent coupling of the polymer provides stable thin polymer films without dewetting during further applications. Stretching and fixing of DNA molecules by using the receding meniscus method is demonstrated. Best DNA binding and stretching was obtained at pH 7.8, without the need for precoating the surface with additional layers of (bio)molecules. In addition, the presented substrates do not require very small volumes of liquids as used in fluid fixation methods and therefore obviate the need for spotting instrumentation.

2. EXPERIMENTAL SECTION

2.1. Materials. Poly(maleic anhydride-*alt*-1-octadecene) (PMAOD, M_w 30,000−50,000 g/mol), 3-aminopropyl triethoxysilane (APTES), and *N*,*N*-diisopropylethylamine (DIPEA) were obtained from Sigma-Aldrich. λ-DNA (48,502bp) was purchased from New England Biolabs. YOYO-1 was purchased from Molecular Probes (Life Technologies, Singapore). Tris-EDTA buffer was obtained from Life Technologies, Singapore. Potassium hydroxide (KOH) and anhydrous tetrahydrofuran (THF) were obtained from Merck. Solvents including acetone, ethanol, and isopropyl alcohol were purchased from Tedia Company, Inc. Milli-Q water (18MΩ) was used to prepare all aqueous solutions for the experiments.

2.2. Preparation of PMAOD Thin Films on Glass Surface. Glass coverslips were cleaned by successive sonication in 1 M KOH, ethanol, and acetone for 10 min each for a total of three cycles. Then the coverslips were rinsed with Milli-Q water and acetone and dried under N_2. After cleaning, the coverslips were incubated in APTES solution (2% v/v in acetone) for 30 min. The silanization reaction was quenched by adding large amounts of water. Coverslips were then rinsed with copious amounts of water and dried under N_2. APTES-coated coverslips were subsequently reacted with 180 mg of PMAOD in the presence of 200 μL of a Hünig's base (DIPEA) dissolved in 10 mL of THF solution for different times. After functionalization, the coverslips were carefully rinsed with THF, acetone, and Milli-Q water and dried with nitrogen gas.

2.3. Staining λ-DNA with YOYO-1. λ-DNA was first diluted with 10 mM Tris-EDTA buffer solution (at pH = 5.5, 7.8, and 8.9) to a concentration of 5 μg/mL. YOYO-1 (1 mM in DMSO) was diluted to a 100 nM stock solution. To stain the DNA molecules, different amounts of DNA and YOYO-1 solutions were taken for staining at various dye to base pair ratios of 1:5, 1:25, and 1:50. To achieve homogeneous staining, the mixtures of YOYO-1 and DNA were further incubated for 1 h at room temperature in the dark.

2.4. Characterization of the PMAOD-Coated Surface. *Contact Angle Goniometry.* The static contact angles were measured at room temperature using an NRL contact angle goniometer (Model 100-00, Rame-Hart, Inc.) equipped with a video camera. Using an autodispenser, three 4 μL water droplets were placed at various places on the substrate, and an average contact angle read on both sides of the droplet using DROPimage Advanced software is reported (±3°).

Ellipsometry. The thickness of polymer film was measured by a high-speed monochromator system (HS-190, J. A. Woollam Co. Inc.) equipped with a 75W light source. All the measurements were carried out at an angle of incidence of 65°.

Fourier Transform Infrared (FTIR) Spectroscopy. FTIR spectra were measured on a Perkin-Elmer Spectrum 2000 FTIR spectrometer. KBr pallets were used for powder PMAOD measurement. Attenuated Total Reflectance Fourier Transform Infrared (ATR-FTIR) spectra were collected at an incidence angle of 60° with a resolution of 4 cm^{-1}. A blank SiO_2 substrate was used for background measurements.

Atomic Force Microscopy (AFM). AFM topography measurements were performed with a Veeco Bioscope II Atomic Force Microscope, equipped with a Nano Scope IIIa controller, in the tapping mode using standard single beam silicon cantilevers with a nominal spring constant of 42 nN/nm (Nanosensors, Germany). All experiments were performed under ambient conditions in air. From the height image the arithmetic average roughness defined as

$$R_a = \frac{1}{n}\sum |Z_i| \tag{1}$$

and the root mean squared surface roughness defined as

$$R_q = \sqrt{\frac{\Sigma z_i^2}{n}} \tag{2}$$

were obtained. In eqs 1 and 2, n is the number of points on the image, and Z is the height deviation measured from a mean plane.

X-ray Photoelectron Spectroscopy (XPS). The analysis of the samples was carried out using a Thermo Scientific Theta Probe XPS. Monochromatic Al K_α X-ray source ($h\nu$ = 1486.6 eV) for analysis at an incident angle of 30° with respect to the surface normal was employed. Photoelectrons were collected at a takeoff angle of 50° with respect to the surface normal. The analysis area was approximately 400 μm in diameter. Survey spectra and high-resolution spectra were acquired for surface elemental identification. The spectral deconvolution was performed by a curve-fitting procedure based on Lorentzian functions broadened by a Gaussian function using the manufacturer's standard software. Charge compensation was performed by means of low-energy electron flooding, and further correction was made based on adventitious C 1s peak at 285.0 eV using the manufacturer's standard software. The error of binding energy determination is estimated to be within ±0.2 eV.

2.5. Imaging of Stained λ-DNA by Wide-Field Microscopy. Samples for imaging were prepared at 25 °C by depositing 1 μL solutions of DNA onto glass cover slides coated with APTES or PMAOD. Fluorescence imaging of individual stained λ-DNA was performed with a custom wide-field microscope (WFM) based on a Nikon ECLIPSE Ti−U inverted microscope frame. Light from a CW multiline Ar ion laser (λ_{ex} = 488 nm, Melles Griot, CA, USA) was fiber-coupled to a Nikon TIRF attachment and after passing through an excitation filter (z488/10×) it was reflected from a dichroic mirror (Z488RDC) and focused on the back aperture of a high NA objective (Nikon TIRF Apo, 100×, NA = 1.49, oil immersion). Immersion oil (n_D = 1.4790, Cargille, USA) was added between the high NA objective and the coverslip for index matching. The luminescence was collected by the same objective, and after passing through the dichroic mirror and the emission filter (HQ500LP) it was directed onto an iXonEM+897 EMCCD camera (512 × 512 pixels, 150 nm per pixel resolution, Andor Technology, Northern Ireland) connected to the side port of the microscope. The camera was connected to a computer furbished with camera-dedicated software to control the imaging parameters and for data acquisition. The experiments were performed in air under ambient conditions. Single DNA diffusion in solution and during meniscus drying were continuously imaged with 100 ms time resolution. The length of individual DNA chains was obtained using routines incorporated into NIS Elements Ar 4.10.00 (Nikon, Japan) software. Statistical analysis of the data was performed using OriginPro8 software (OriginLab Corporation, USA).

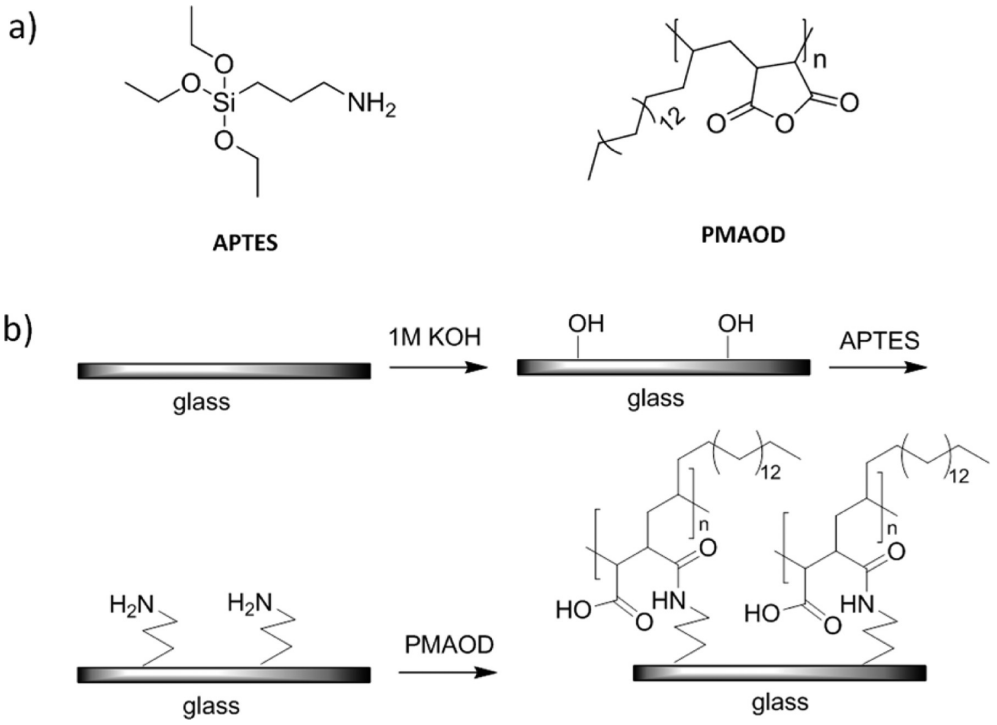

Figure 1. a) Chemical structures of APTES and PMAOD. b) Scheme of the functionalization of the glass slides with APTES and PMAOD.

3. RESULTS AND DISCUSSION

PMAOD-coated glass slides were prepared by reacting the maleic anhydride units located along the PMAOD backbone (Figure 1a) with amine-derivatized glass slides. The amine functionality on the glass surface was introduced by silanization of freshly cleaned glass slides with 3-aminopropyl triethoxysilane (APTES) (Figure 1b). To ensure good APTES coupling, the glass slides have to be degreased and activated with functional groups able to react with the ethoxysilane groups. We have adopted a cleaning procedure involving sonication in KOH, ethanol, and acetone, which reproducibly rendered the substrate highly hydrophilic, characterized by contact angles below 10°. The silanization was performed in solution. Within the first 30 min of silanization the contact angle increased sharply to above 45° (Figure 2), a value expected for NH_2-functionalized surface,[32,33] indicating coupling of the silanes to glass. Reaction times up to 2 h did not influence substantially the contact angles. However, reactions longer than 120 min often resulted in surfaces with lower contact angles. This is likely due to APTES polymerization, aggregation, and thicker film formation.[32]

PMAOD is a hydrophobic polymer which is not soluble directly in water but dissolves well in organic solvents such as THF. We have performed the coupling reaction of PMAOD to amine-functionalized glass slides directly in THF in the presence of a Hünig's base, *N*,*N*-diisopropylethylamine (DIPEA), as the catalyst. DIPEA is an effective catalyst and easily induces phase transfer of PMAOD from THF to water by catalyzing the hydrolysis of the anhydride units to carboxylic acids. The comparison of contact angles between clean glass, APTES coated glass, and PMAOD coated glass is shown in Figure 2.

XPS results for APTES-coated glass reveal single peaks in the N 1s, O 1s, and C 1s regions (Figure 3). XPS of PMAOD-coated glass confirms the presence of new carbon species with

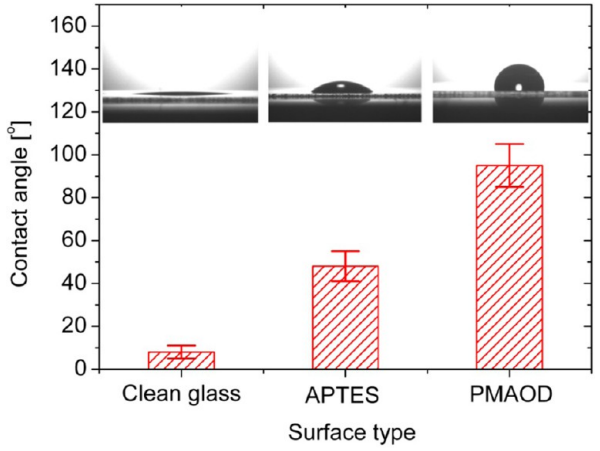

Figure 2. Comparison between the contact angles for clean glass cover slides, APTES functionalized slides, and APTES slide after coupling with PMAOD. The insets show photographs of water droplets deposited on each surface.

distinct signatures of O═C−O−C═O anhydride units. In particular, the new O 1s peak at 532.8 eV with concurrent emergence of a C 1s peak at 289.6 clearly indicates the presence of the anhydride, while the C 1s peak at 288.6 eV is attributed to an N−C═O carbon indicating amide formation. The new nitrogen peak at 402.1 eV also indicates the formation of amide bonds between the polymer and the APTES-coated surface. In addition, FTIR spectrum of the PMAOD-coated surface gives evidence of the amide bond formation. After functionalization of PMAOD, a new peak at 1681 cm^{-1} attributed to amide bond stretching is clearly observable, indicating covalent coupling of PMAOD to APTES (see the Supporting Information).

The thickness of the dry PMAOD film as measured by ellipsometry was equal to 2.0 ± 0.5 nm. AFM imaging revealed that the surface of PMAOD-coated slides displayed a micellar-

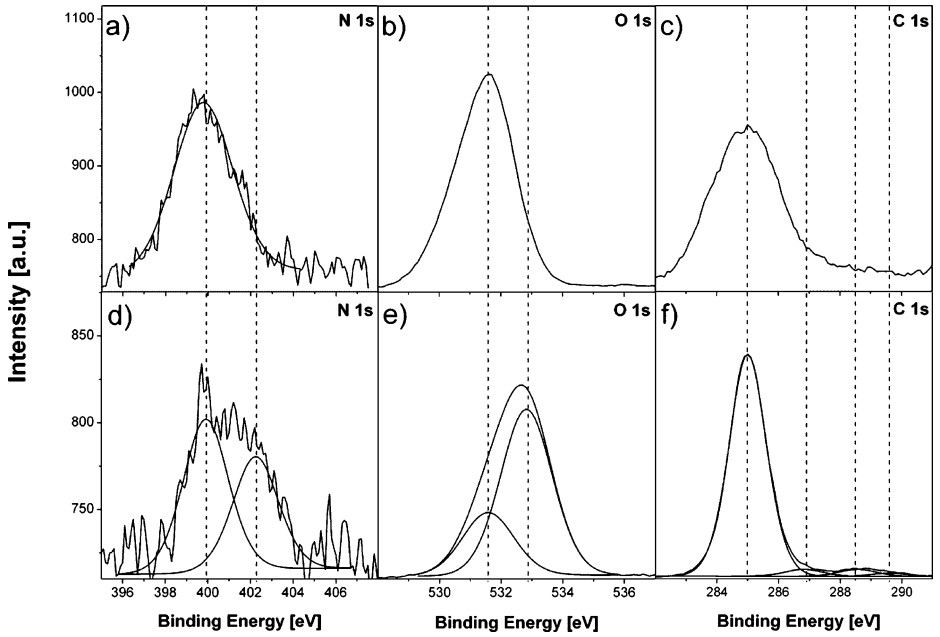

Figure 3. XPS spectra for N 1s, O 1s, and C 1s regions for APTES (a-c) and PMAOD (d-f) coated glass slide.

like morphology (Figure 4a) and that the surface roughness decreased as a function of reaction time (Figure 4b). Taking into account the value of the film thickness measured by ellipsometry and the observed surface morphology we hypothesize that the morphology of the PMAOD films is the result of a micellar morphology of the polymer already in THF solution due to the presence of partially hydrolyzed anhydride units, which would result in a mildly amphiphilic character of the polymer in THF and the polymer adopting a micelle-like conformation. As a corroborating evidence, FTIR of the PMAOD powder (see the Supporting Information) shows the presence of two bands at 1857 and 1781 cm^{-1} attributed to the asymmetric carbonyl stretching of the cyclic anhydride but also a carbonyl stretching band at 1712 cm^{-1} resulting from partial hydrolysis of PMAOD to carboxylic acids.[30,34]

The contact angles of the PMAOD coated glass were found to be above 90° confirming previously reported results that the wettability of this type of polymers is primarily controlled by the alkyl side chain. Thus, the hydrophobicity of the PMAOD layer is reminiscent to that of polyethylene brushes (CA = 104°)[35] or CH_3 terminated surface monolayers.[36]

Prior to performing the DNA stretching experiments, we first stained DNA molecules with a fluorescent dye. YOYO-1 was chosen as it has a large molar absorptivity and high binding constant to double-stranded DNA (dsDNA), and it shows little fluorescence in free form but exhibits strong fluorescence enhancement after binding to dsDNA.[28,37,38] The latter property allows for efficient visualization of single DNA chains while keeping the background luminescence low. To check the effect of the staining on DNA stretching, λ-DNA was stained at various dye-to-base pair ratios of 1:5, 1:25, and 1:50. After staining, the λ-DNA solution was deposited on the PMAOD glass surface and imaged by wide-field microscopy. We have explored different deposition methods and surface and solution conditions. By far the best results were obtained by depositing a droplet of the DNA solution on the sample and stretching the DNA by the receding meniscus of the evaporating droplet. When using an NH_2-coated glass slide as control, we noticed that the DNA immediately adsorbs to the substrate resulting in fluorescence images with strongly emitting surface-bound spots (Figure 5). This is likely due to electrostatic interactions between negatively charged DNA and positively charged, partially protonated amine groups on the surface. Such strongly adsorbed DNA could not be stretched anymore by the receding droplet meniscus at any pH conditions. The adsorption of λ-DNA to the surface was drastically reduced when PMAOD was introduced. The hydrophobic nature of the surface (concurrently with possible negatively charged carboxylic groups from the hydrolyzed anhydride) prevented the absorption of negatively charged DNA. At pH =7.8, when the contact line between the deposited droplet and the surface started to move due to the evaporation of the droplet, stretching of the DNA could be clearly observed (Figure 6a,b,c) normal to the contact line of the receding droplet. The mechanism for the stretching is unclear, but it is believed to involve first a preferential adsorption of DNA chain ends and then uncoiling and stretching of the DNA chains in solution before the other end sticks to the surface. The hydrodynamic forces generated near the solid−liquid interface are apparently strong enough to overcome the entropic resistance to molecular extension, affording elongated DNA strands.[19] It should be noted, that the DNA stretching was optimal at pH = 7.8. Stretching of DNA at a lower pH = 5.5 resulted in higher DNA adsorption to the substrate and ill-defined stretched DNA chains, presumably due to the protonation of the DNA and high nonspecific adsorption of the DNA to the surface (Figure s-2). Stretching of the DNA at a higher pH = 8.9 resulted in the formation of fiber-like DNA structures (instead of individual DNA chains) (Figure s-3).[39]

For the well-stretched DNA at pH = 7.8 we have quantified the degree of elongation by measuring the length of the stretched strands directly from the wide field fluorescence images. In particular, we have compared the degree of stretching of DNA on PMAOD as a function of the staining ratio (1:50, 1:25, and 1:5). First, we note that the staining ratio directly influences the brightness of the DNA on the surface and clearly the DNA stained at the 1:5 ratio results in much brighter stretched DNA compared to DNA stained at the 1:25

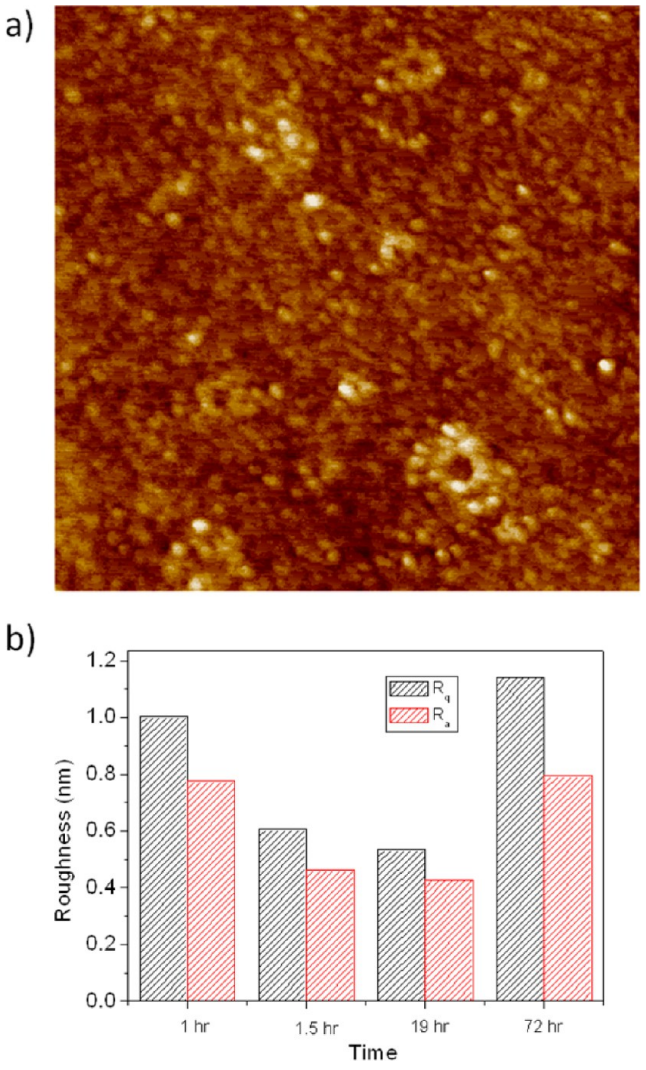

Figure 4. a) AFM height image of PMAOD coated glass slide after 2 h reaction time. The scan size is 1 × 1 μm^2, and the z-scale range is 3.54 nm. b) Roughness parameters R_a and R_q for the PMAOD coated glass as a function of the reaction time.

and 1:50 ratios. For dsDNA stained at a larger dye-to-DNA base pair ratio, more dye molecules are intercalated in the dsDNA conferring higher fluorescence. Second, the degree of stretching is not uniform for all DNA chains and the DNA

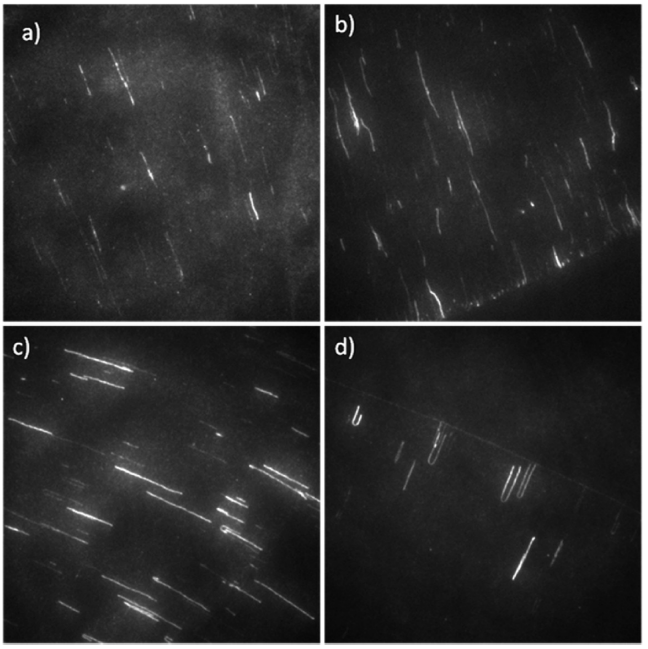

Figure 6. Representative fluorescence images of stretched λ-DNA on the PMAOD surface and stained at (a) 1:50, (b) 1:25, and (c,d) 1:5 dye to base pair ratios at pH 7.8. The U-shaped stretched λ-DNA (d) could be found close to the droplet initial contact line for DNA stained at 1:5 dye to base pair ratio. Image size is 80 μm.

length after stretching varies. This may be due to slightly different points of attachment or varying magnitudes of stretching forces along the chain direction.

We have plotted the measured DNA length data normalized by the unstained DNA contour length found in the literature (16.2 μm).[40,41] (We explicitly assume here that the real DNA length distribution is monodisperse, i.e., all chains have the same length, but we cannot exclude the possibility that some of the chains break during staining or elongation.) The histograms of DNA stretching ratio shown in Figure 7 confirm the broad distribution of the stretching lengths and suggest that the stretching of DNA molecules is comparable for the different staining ratios. The majority of DNA molecules were stretched from 0.4 to 1.2 of their contour length.

For the larger staining ratios the contribution of DNA stretched beyond their contour length increases, and a noticeable peak at 1.1 for the staining ratio of 1:5 appears. The degree of stretching of the DNA can be affected by the

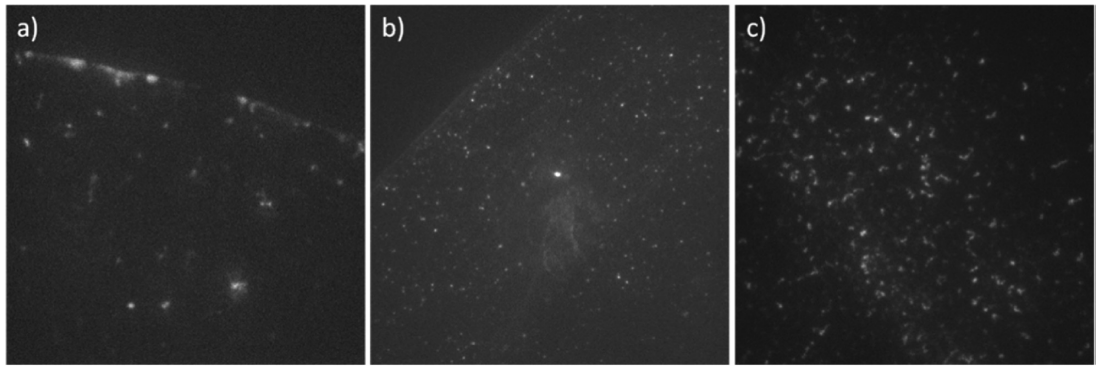

Figure 5. Fluorescence images of λ-DNA deposited on NH_2 coated surface under pH 5.5 (a), pH 7.8 (b), and pH 8.9 (c). Note the droplet contact line visible in a) and b). Image size is 80 μm.

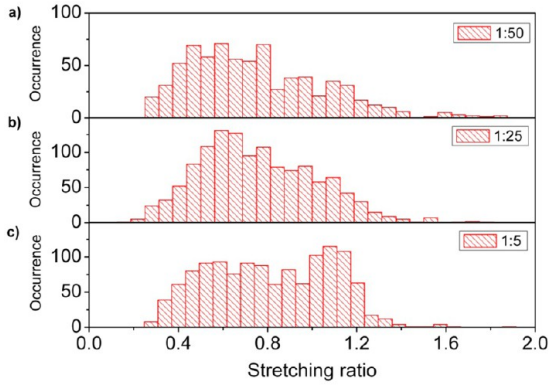

Figure 7. Histograms of the λ-DNA stretching ratios for DNA stained with YOYO-1 at different dye to base pair ratio of (a) 1:50, (b) 1:25, and (c) 1:5. Although the distributions of the stretching ratios are broad, the number of DNA molecule stretched beyond their contour length increases for higher staining ratios and a clear peak appears in the distribution for the 1:5 staining.

presence of the intercalating probe, and it also depends on the magnitude of the hydrodynamic force. For equal hydrodynamic force acting on the DNA, a larger staining ratio would result in longer DNA chains visible in the fluorescence images, in line with the results shown in Figure 7.

We would like to stress that the observed DNA stretching can be obtained for relatively large droplet sizes (several millimeters), and therefore when using PMAOD-coated surfaces one does not require small volume spotting machines. Interestingly, we have also observed that for the 1:5 staining ratio, the λ-DNA close to the original contact line (formed after droplet deposition) stretched into a characteristic U-shape (Figure 6d). Observation of such shapes is in line with the DNA chain-end attachment model, but in this case both chain ends were stuck to the surface before the meniscus started to recede.

4. CONCLUSIONS

We have presented an easy and robust surface functionalization method for efficient deposition and stretching of dsDNA chains. Hydrophobic surfaces characterized by high contact angles (CA > 90°) were obtained by covalently grafting poly(maleic anhydride-*alt*-1-octadecene) (PMAOD) to amine functionalized glass surface. The coupling was evidenced by the appearance of new peaks on the XPS spectrum in the nitrogen, oxygen, and carbon regions. The thin film nanoscale morphology, as imaged by AFM, and the film thickness obtained by ellipsometry indicate that the globular-like surface features are due to coupling of partially hydrolyzed PMAOD micelles to the surface. This interesting point will be addressed more in depth in a future contribution. The receding meniscus method was used for stretching coiled λ-DNA strands. Compared to amine-functionalized surface, where no stretching was observed, stretching of dsDNA on the PMAOD surface was efficient and reproducible with best results obtained at pH 7.8. The amount of YOYO-1 dye used to stain the DNA had a minor effect on the overall stretching length distributions; however, for high dye to base pair ratios a clear peak for stretching close to the contour length of the DNA is observed.

■ ASSOCIATED CONTENT

Supporting Information

ATR-FTIR spectra of the PMAOD powder and the PMAOD functionalized surface, representative fluorescence images for DNA stretching at pH 5.5 and 8.9 on the PMAOD surface. This material is available free of charge via the Internet at http://pubs.acs.org.

■ AUTHOR INFORMATION

Corresponding Author

*Phone: +65 6874 8357. Fax: +65-6774 4657. E-mail: tomczakn@imre.a-star.edu.sg.

Notes

The authors declare no competing financial interest.

■ ACKNOWLEDGMENTS

We are grateful to the Institute of Materials Research and Engineering, A*STAR (Agency for Science, Technology and Research) and the A*STAR Joint Council Office (Grant 10/03/FG/06/07) for providing financial support.

■ REFERENCES

(1) Strick, T. R.; Allemand, J.-F.; Bensimon, D.; Bensimon, A.; Croquette, V. The Elasticity of a Single Supercoiled DNA Molecule. *Science* **1996**, *271*, 1835−1837.

(2) Smith, S. B.; Cui, Y. J.; Bustamante, C. Overstretching B-DNA: The Elastic Response of Individual Double-Stranded and Single-Stranded DNA Molecules. *Science* **1996**, *271*, 795−799.

(3) Perkins, T. T.; Quake, S. R.; Smith, D. E.; Chu, S. Relaxation of a Single DNA Molecule Observed by Optical Microscopy. *Science* **1994**, *264*, 822−826.

(4) Perkins, T. T.; Smith, D. E.; Chu, S. Direct Observation of Tube-like Motion of a Single Polymer-Chain. *Science* **1994**, *264*, 819−822.

(5) Cluzel, P.; Lebrun, A.; Heller, C.; Lavery, R.; Viovy, J. L.; Chatenay, D.; Caron, F. DNA: An Extensible Molecule. *Science* **1996**, *271*, 792−794.

(6) Perkins, T. T.; Smith, D. E.; Larson, R. G.; Chu, S. Stretching of a Single Tethered Polymer in a Uniform-Flow. *Science* **1995**, *268*, 83−87.

(7) Gueroui, Z.; Place, C.; Freyssingeas, E.; Berge, B. Observation by Fluorescence Microscopy of Transcription on Single Combed DNA. *Proc. Natl. Acad. Sci. U.S.A.* **2002**, *99*, 6005−6010.

(8) Bustamante, C.; Smith, S. B.; Liphardt, J.; Smith, D. Single-Molecule Studies of DNA Mechanics. *Curr. Opin. Struct. Biol.* **2000**, *10*, 279−285.

(9) Kim, J. H.; Dukkipati, V. R.; Pang, S. W.; Larson, R. G. Stretching and Immobilization of DNA for Studies of Protein-DNA Interactions at the Single-Molecule Level. *Nanoscale Res. Lett.* **2007**, *2*, 185−201.

(10) Kim, J. H.; Shi, W.-X.; Larson, R. G. Methods of Stretching DNA Molecules Using Flow Fields. *Langmuir* **2007**, *23*, 755−764.

(11) Levy-Sakin, M.; Ebenstein, Y. Beyond Sequencing: Optical Mapping of DNA in the Age of Nanotechnology and Nanoscopy. *Curr. Opin. Biotechnol.* **2013**, *24*, 690−698.

(12) Weier, H. U. G.; Wang, M.; Mullikin, J. C.; Zhu, Y.; Cheng, J.-F.; Greulich, K. M.; Bensimon, A.; Gray, J. W. Quantitative DNA Fiber Mapping. *Hum. Mol. Genet.* **1995**, *4*, 1903−1910.

(13) Michalet, X.; Ekong, R.; Fougerousse, F.; Rousseaux, S.; Schurra, C.; Hornigold, N. Dynamic Molecular Combing: Stretching the Whole Human Genome for High-resolution Studies. *Science* **1997**, *277*, 1518−1523.

(14) Cai, W. W.; Jing, J. P.; Irvin, B.; Ohler, L.; Rose, E.; Shizuya, H.; Kim, U. J.; Simon, M. High-Resolution Restriction Maps of Bacterial Artificial Chromosomes Constructed by Optical Mapping. *Proc. Natl. Acad. Sci. U.S.A.* **1998**, *95*, 3390−3395.

(15) Cai, W. W.; Aburatani, H.; Stanton, V. P.; Housman, D. E.; Wang, Y. K.; Schwartz, D. C. Ordered Restriction-Endonuclease Maps

of Yeast Artificial Chromosomes Created by Optical Mapping on Surfaces. *Proc. Natl. Acad. Sci. U.S.A.* **1995**, *92*, 5164−5168.
(16) Meng, X.; Benson, K.; Chada, K.; Huff, E. J.; Schwartz, D. C. Optical Mapping of Bacteriophage-lambda Clones Using Restriction Endonucleases. *Nat. Genet.* **1995**, *9*, 432−438.
(17) Jing, J.; Reed, J.; Huang, J.; Hu, X.; Clarke, V.; Edington, J.; Housman, D.; Anantharaman, T. S.; Huff, E. J.; Mishra, B.; Porter, B.; Shenker, A.; Wolfson, E.; Hiort, C.; Kantor, R.; Aston, C.; Schwartz, D. C. Automated High Resolution Optical Mapping Using Arrayed, Fluid-Fixed DNA Molecules. *Proc. Natl. Acad. Sci. U.S.A.* **1998**, *95*, 8046−8051.
(18) Yokota, H.; Johnson, F.; Lu, H. B.; Robinson, R. M.; Belu, A. M.; Garrison, M. D.; Ratner, B. D.; Trask, B. J.; Miller, D. L. A New Method for Straightening DNA Molecules for Optical Restriction Mapping. *Nucleic Acids Res.* **1997**, *25*, 1064−1070.
(19) Dorfman, K. D.; King, S. B.; Olson, D. W.; Thomas, J. D. P.; Tree, D. R. Beyond Gel Electrophoresis: Microfluidic Separations, Fluorescence Burst Analysis, and DNA Stretching. *Chem. Rev.* **2013**, *113*, 2584−2667.
(20) Bensimon, A.; Simon, A.; Chiffaudel, A.; Croquette, V.; Heslot, F.; Bensimon, D. Alignment and Sensitive Detection of DNA by a Moving Interface. *Science* **1994**, *265*, 2096−2098.
(21) Bensimon, D.; Simon, A. J.; Croquette, V.; Bensimon, A. Stretching DNA with a Receding Meniscus: Experiments and Models. *Phys. Rev. Lett.* **1995**, *74*, 4754−4757.
(22) Hu, J.; Wang, M.; Weier, H.-U. G.; Frantz, P.; Kolbe, W.; Ogletree, D. F.; Salmeron, M. Imaging of Single Extended DNA Molecules on Flat (Aminopropyl)triethoxysilane-mica by Atomic Force Microscopy. *Langmuir* **1996**, *12*, 1697−1700.
(23) Allemand, J.-F.; Bensimon, D.; Jullien, L.; Bensimon, A.; Croquette, V. pH-Dependent Specific Binding and Combing of DNA. *Biophys. J.* **1997**, *73*, 2064−2070.
(24) Schwartz, D. C.; Li, X.; Hermandez, L.; Ramnarain, S. P.; Huff, E. J.; Wang, Y. K. Ordered Restriction Maps of Saccharomyces-cerevisiae Chromosomes Constructed by Optical Mapping. *Science* **1993**, *262*, 110−114.
(25) Nakao, H.; Hayashi, H.; Yoshino, T.; Sugiyama, S.; Otobe, K.; Ohtani, T. Useful Technique for DNA-stretching and Fixation. *Nucleic Acids Res.* **2002**, No. Supplement No. 2, 289−290.
(26) Matsuoka, T.; Kim, B. C.; Huang, J. X.; Douville, N. J.; Thouless, M. D.; Takayama, S. Nanoscale Squeezing in Elastomeric Nanochannels for Single Chromatin Linearization. *Nano Lett.* **2012**, *12*, 6480−6484.
(27) Dimalanta, E. T.; Lim, A.; Runnheim, R.; Lamers, C.; Churas, C.; Forrest, D. K.; de Pablo, J. J.; Graham, M. D.; Coppersmith, S. N.; Goldstein, S.; Schwartz, D. C. A Microfluidic System for Large DNA Molecule Arrays. *Anal. Chem.* **2004**, *76*, 5293−5301.
(28) Namasivayam, V.; Larson, R. G.; Burke, D. T.; Burns, M. A. Electrostretching DNA Molecules using Polymer-enhanced Media within Microfabricated Devices. *Anal. Chem.* **2002**, *74*, 3378−3385.
(29) Pompe, T.; Salchert, K.; Alberti, K.; Zandstra, P.; Werner, C. Immobilization of Growth Factors on Solid Supports for the Modulation of Stem Cell Fate. *Nat. Protoc.* **2010**, *5*, 1042−1050.
(30) Schmidt, U.; Zschoche, S.; Werner, C. Modification of Poly(octadecene-*alt*-maleic anhydride) Films by Reaction with Functional Amines. *J. Appl. Polym. Sci.* **2003**, *87*, 1255−1266.
(31) Beyer, D.; Bohanon, T. M.; Knoll, W.; Ringsdorf, H.; Elender, G.; Sackmann, E. Surface Modification via Reactive Polymer Interlayers. *Langmuir* **1996**, *12*, 2514−2518.
(32) Kim, J.; Seidler, P.; Wan, S. W.; Fill, C. Formation, Structure, and Reactivity of Amino-Terminated Organic Films on Silicon Substrates. *J. Colloid Interface Sci.* **2009**, *329*, 114−119.
(33) Zeng, X.; Xu, G.; Gao, Y.; An, Y. Surface Wettability of (3-Aminopropyl)triethoxysilane Self-Assembled Monolayers. *J. Phys. Chem. B* **2011**, *115*, 450−454.
(34) Pompe, T.; Zschoche, S.; Herold, N.; Salchert, K.; Gouzy, M. F.; Sperling, C.; Werner, C. Maleic Anhydride Copolymers - A Versatile Platform for Molecular Biosurface Engineering. *Biomacromolecules* **2003**, *4*, 1072−1079.
(35) Damiron, D.; Mazzolini, J.; Cousin, F.; Boisson, C.; D'Agosto, F. Poly(ethylene) Brushes Grafted to Silicon Substrates. *Polym. Chem.* **2012**, *3*, 1838−1845.
(36) Ishizaki, T.; Saito, N.; SunHyung, L.; Ishida, K.; Takai, O. Study of Alkyl Organic Monolayers with Different Molecular Chain Lengths Directly Attached to Silicon. *Langmuir* **2006**, *22*, 9962−9966.
(37) Glazer, A. N.; Rye, H. S. Stable Dye-DNA Intercalation Complexes as Reagents for High-Sensitivity Fluorescence Detection. *Nature* **1992**, *359*, 859−861.
(38) Shimizu, M.; Sasaki, S.; Tsuruoka, M. DNA Length Evaluation using Cyanine Dye and Fluorescence Correlation Spectroscopy. *Biomacromolecules* **2005**, *6*, 2703−2707.
(39) Li, B.; Han, W.; Byun, M.; Zhu, L.; Zou, Q.; Lin, Z. Macroscopic Highly Aligned DNA Nanowires Created by Controlled Evaporative Self-Assembly. *ACS Nano* **2013**, *7*, 4326−4333.
(40) Bjork, P.; Holmstrom, S.; Inganas, O. Soft Lithographic Printing of Patterns of Stretched DNA and DNA/electronic Polymer Wires by Surface-Energy Modification and Transfer. *Small* **2006**, *8*, 1068−1074.
(41) Guan, J.; Lee, L. J. Generating Highly Ordered DNA Nanostrand Arrays. *Proc. Natl. Acad. Sci. U.S.A.* **2005**, *102*, 18321−18325.